Cilia Transport for Micropolar Fluid Through a Uniform Cylindrical Tube

[1,2]Y. Abd Elmaboud and [1,3]Tarek G. Emam

[1]Mathematics Department
Faculty of Science and Arts
Khulais, University of Jeddah
Saudi Arabia

[2]Mathematics Department
Faculty of Science
Al-Azhar University (Assiut Branch)
Assiut, Egypt
yass_math@yahoo.com

[3]Mathematics Department
Faculty of Science
Ain-Shams University
Cairo, Egypt
tarek.emam@sci.asu.edu.eg

Abstract

The aim of this work is to study the role that the cilia motion plays in the transport of a micropolar fluid in a uniform cylindrical tube. The transport due to systems of beating cilia is responsible for the transport of bio-fluids in numerous physiological processes. Cylindrical coordinates are used to formulate the system of equations with the suitable boundary conditions governing the flow. Such system is then simplified through considering the long wavelength and low Reynolds number assumptions. Solutions are found for the velocity components, the pressure gradient, and the stream function which include many parameters such as the cilia length parameter, the eccentricity parameter of the elliptical motion and the wave number. The results shows that the pumping machinery functions more efficiently to push ahead micropolar fluid than Newtonian fluid. The obtained results may help to understand more the processes of the transport of bio-fluids in human body.

1. Introduction

The study of the processes of transport of bio-fluids inside the human body has attracted many researchers in recent years. One of these processes is the transport due to systems of beating cilia. Cilia are a minor hair beat in rhythmic waves and it is responsible for the transport of bio-fluids in numerous physiological processes like the motion of epididymal fluid in the efferent ductus of the human male reproductive tract and the removal of tracheobronchial mucus in the respiratory track, the transport of ovulatory mucus and ovum in the oviduct of the female reproductive tract system. In the literature there are numerous theoretical investigations in cilia transport. Lardner and Shack (1972) have studied the mathematical model of cilia transport in the duetus efferentes of the male reproductive tract. After this investigation several theoretical and experimental studies have been presented to understand cilia transport. Agarwal and Anwaruddin (1984) have discussed the effect of variable viscosity on the fluid transported by cilia. The investigation of a power law fluid in the channel with ciliated walls has been presented by Siddiqui et al. (2010). Siddiqui et al. ((2014 a) and (2014 b)) have considered the MHD effect on the fluid flow by cilia in a channel and tube respectively. The rheological of power law fluid flows in a tube by metachronal wave of cilia has been discussed by Maiti and Pandey (2017).

The Navier-Stokes model of hydrodynamics has a radical restriction. It can't depict fluids with microstructure and complex liquids. Eringen (1966) has introduced a mathematical model of fluid (micropolar fluid) comprising of rigid, randomly oriented particles suspended in a viscous medium. Microfluidics deal with the flow of liquids inside a micrometer-sized channels. Microfluidics have many applications such as water purification and genetics research. Many researchers have used the model established by Eringen to describe some biological problems. Srinivasacharya et al. (2003) have discussed the peristaltic flow of a micropolar fluid in a tube. The heat transfer distribution through a micropolar fluid in a porous channel with peristalsis has been introduced by Abd elmaboud (2011). Abd elmaboud (2013) has also studied the effect of peristaltic transport and heat transfer of a magneto micropolar fluid through porous channel. Vijaya et al. (2016) have discussed the effects of both stenosis and post stenotic dilatation on steady flow of micropolar fluid through an artery.

With the above discussion in mind, the goal of this investigation is to formulate and solve the mathematical model which describe the transport due to systems of beating cilia for a micropolar fluid. We study the effects of micropolar parameters as well as cilia transport parameters on the fluid motion. Cylindrical coordinates are used to formulate the system of equations with the suitable boundary conditions governing the flow. Solutions are found for the velocity components, the pressure gradient, and the stream function which include many parameters such as the cilia length parameter, the eccentricity parameter of the elliptical motion and the wave number.

2. Formulation of the problem

Consider a micropolar fluid in an infinite circular tube ciliated with metachronal waves. The movement of the fluid occurs due to aggregate beating of the cilia. The model of the problem is shown in figure 1. We can express mathematically the envelopes of the cilia tips as

$$R' = H' = a + b\cos\left(\frac{2\pi}{\lambda}(Z' - ct')\right) \tag{1}$$

$$Z' = g'(Z', Z'_0, t') = Z'_0 + b\alpha \sin\left(\frac{2\pi}{\lambda}(Z' - ct')\right), \tag{2}$$

where a is the radius of the tube, $b = a\varepsilon$ is the wave amplitude, ε is a non-dimensional measure with respect to the cilia length, α is a measure of the eccentricity of the elliptical motion, Z'_0 is a reference position, λ is the wavelength, c is the propagation velocity, and t' is time.

In case of no-slip condition applied to the tube wall, the velocities conferred to fluid particles are just those of the cilia tips. To get the horizontal and radial velocities of the cilia we have

$$V'_z = \frac{\partial Z'}{\partial t'}\Big|_{z'_0} = \frac{\partial g'}{\partial t'} + \frac{\partial g'}{\partial Z'}\frac{\partial Z'}{\partial t'} = \frac{\partial g'}{\partial t'} + \frac{\partial g'}{\partial Z'}V'_z, \tag{3}$$

$$V'_r = \frac{\partial R'}{\partial t'}\Big|_{z'_0} = \frac{\partial H'}{\partial t'} + \frac{\partial H'}{\partial Z'}\frac{\partial Z'}{\partial t'} = \frac{\partial H'}{\partial t'} + \frac{\partial H'}{\partial Z'}V'_z, \tag{4}$$

with help of equations (1-2) we get

$$V'_z = \frac{\dfrac{-2\pi}{\lambda}(\alpha\varepsilon ac\cos(\dfrac{2\pi}{\lambda})(Z'-ct'))}{1 - \dfrac{2\pi}{\lambda}(\alpha\varepsilon a\cos(\dfrac{2\pi}{\lambda})(Z'-ct'))}, \tag{5}$$

$$V'_r = \frac{\dfrac{2\pi}{\lambda}(\alpha\varepsilon ac\sin(\dfrac{2\pi}{\lambda})(Z'-ct'))}{1 - \dfrac{2\pi}{\lambda}(\alpha\varepsilon a\cos(\dfrac{2\pi}{\lambda})(Z'-ct'))}. \tag{6}$$

The fluid is unsteady in the fixed frame (R', Z'). We introduce a new frame (r', z') moving with velocity c in which the fluid is steady. The transformation between the two frames are

$$z' = Z' - ct, \quad r' = R', \quad v'_z = V'_z - c, \quad v'_r = V'_r, \tag{7}$$

where (v'_r, v'_z) denotes the radial and the axial velocity in the moving frame respectively. Using the transformation (7) the system of equations governing the steady flow of an incompressible micropolar fluid takes the form:

$$\nabla \cdot v' = 0, \tag{8}$$

$$\rho(v' \cdot \nabla v') = -\nabla p' + k \nabla \times w' + (\mu + k)\nabla^2 v', \tag{9}$$

$$\rho j'(v' \cdot \nabla w') = -2kw' + k \nabla \times v' - \gamma(\nabla \times \nabla \times w') + (\nu + \beta + \gamma)\nabla(\nabla \cdot w'), \tag{10}$$

where v' and w' are the velocity and the microrotation vectors respectively, p' is the fluid pressure, ρ and j' are the fluid density and microgyration parameters. Here for this flow the velocity vector is given by $v' = (v_r', 0, v_z')$, while the microrotation vector is given by $w' = (0, w_\theta', 0)$. Introducing the following dimensionless variables:

$$r = \frac{r'}{a}, \quad z = \frac{z'}{\lambda}, \quad v_z = \frac{v_z'}{c}, \quad v_r = \frac{\lambda v_r'}{c\,a}, \quad w_\theta = \frac{a}{c}w_\theta',$$

$$p = \frac{a^2}{\lambda\mu c}p', \quad t = \frac{c}{\lambda}t', \quad j = \frac{j'}{a^2}, \quad r_1 = \frac{r_1'}{a}. \tag{11}$$

The non-dimensional governing equations (8-10) become

$$\frac{\partial v_r}{\partial r} + \frac{\partial v_z}{\partial z} + \frac{v_r}{r} = 0, \tag{12}$$

$$Re\,\delta^3\left(v_r \frac{\partial v_r}{\partial r} + v_z \frac{\partial v_r}{\partial z}\right) = -\frac{\partial p}{\partial r}$$

$$+ \frac{\delta^2}{1-N}\left(-N\frac{\partial w_\theta}{\partial z} + \frac{\partial^2 v_r}{\partial r^2} + \frac{1}{r}\frac{\partial v_r}{\partial r} - \frac{v_r}{r^2} + \delta^2 \frac{\partial^2 v_r}{\partial z^2}\right), \tag{13}$$

$$Re\,\delta\left(v_r \frac{\partial v_z}{\partial r} + v_z \frac{\partial v_z}{\partial z}\right) = -\frac{\partial p}{\partial z}$$

$$+ \frac{1}{1-N}\left(\frac{N}{r}\frac{\partial(rw_\theta)}{\partial r} + \frac{\partial^2 v_z}{\partial r^2} + \frac{1}{r}\frac{\partial v_z}{\partial r} + \delta^2 \frac{\partial^2 v_z}{\partial z^2}\right), \tag{14}$$

$$\frac{j\,Re\,\delta\,(1-N)}{N}\left(v_r \frac{\partial w_\theta}{\partial r} + v_z \frac{\partial w_\theta}{\partial z}\right)$$

$$= -2w_\theta + \left(\delta^2 \frac{\partial v_r}{\partial z} - \frac{\partial v_z}{\partial r}\right) + \frac{2-N}{m^2}\left(\frac{\partial}{\partial r}\left(\frac{1}{r}\frac{\partial(rw_\theta)}{\partial r}\right) + \delta^2 \frac{\partial^2 w_\theta}{\partial z^2}\right). \tag{15}$$

The corresponding boundary conditions are:

$$v_z = \frac{-2\pi\alpha\varepsilon\delta\cos(2\pi z)}{1-2\pi\alpha\varepsilon\delta\cos(2\pi z)} - 1, w_\theta = 0 \quad at \quad r = h(z) = 1 + \varepsilon\cos(2\pi z),$$

$$\frac{\partial v_z}{\partial r} = 0, \quad w_\theta = 0, \qquad\qquad at \quad r = 0,$$

$$(16)$$

where $\delta = a/\lambda$ is the wave number, $Re = \rho ca/\mu$ is the Reynolds number, $N = k/(\mu+k)$ is the coupling number, $m^2 = a_0^2 k(2\mu+k)/(\gamma(\mu+k))$ is the micropolar parameter.

3. Solution of the problem

To solve this problem we use the long wavelength approximation $\delta \ll 1$ with lubrication approach. Dropping terms of order $Re\delta$ and δ^2 and higher. Equations (12-16) reduce to

$$\frac{\partial v_r}{\partial r} + \frac{\partial v_z}{\partial z} + \frac{v_r}{r} = 0, \tag{17}$$

$$\frac{\partial p}{\partial r} = 0, \tag{18}$$

$$\frac{N}{r}\frac{\partial(rw_\theta)}{\partial r} + \frac{\partial^2 v_z}{\partial r^2} + \frac{1}{r}\frac{\partial v_z}{\partial r} = (1-N)\frac{\partial p}{\partial z}, \tag{19}$$

$$2w_\theta + \frac{\partial v_z}{\partial r} - \frac{2-N}{m^2}\frac{\partial}{\partial r}\left(\frac{1}{r}\frac{\partial(rw_\theta)}{\partial r}\right) = 0. \tag{20}$$

The associated boundary conditions in the moving frame are

$$v_z = \frac{-2\pi\alpha\varepsilon\delta\cos(2\pi z)}{1-2\pi\alpha\varepsilon\delta\cos(2\pi z)} - 1, w_\theta = 0, at \quad r = h(z) = 1 + \varepsilon\cos(2\pi z),$$

$$\frac{\partial v_z}{\partial r} = 0, \qquad\qquad w_\theta = 0, at \quad r = 0,$$

$$(21)$$

From equations (19) and (20) we get,

$$\frac{\partial}{\partial r}\left[r\frac{\partial v_z}{\partial r}+Nrw_\theta-(1-N)\frac{r^2}{2}\frac{dp}{dz}\right]=0.\tag{22}$$

Integrating equation (22) with respect to r we have

$$\frac{\partial v_z}{\partial r}=(1-N)\{\frac{r}{2}\frac{dp}{dz}+\frac{\Omega_1(z)}{r}\}-Nw_\theta.\tag{23}$$

Substituting equation (23) into equation (20), we get,

$$\frac{\partial^2 w_\theta}{\partial r^2}+\frac{1}{r}\frac{\partial w_\theta}{\partial r}-(m^2+\frac{1}{r^2})w_\theta=m^2 A\{\frac{r}{2}\frac{dp}{dz}+\frac{\Omega_1(z)}{r}\},\tag{24}$$

where $A=\dfrac{1-n}{2-n}$. The general solution of equation (24) is

$$w_\theta=\Omega_2(z)I_1(mr)+\Omega_3(z)K_1(mr)-A\{\frac{r}{2}\frac{dp}{dz}+\frac{\Omega_1(z)}{r}\},\tag{25}$$

where I_1 and K_1 are modified Bessel functions of first order, first and second kind, respectively. Substituting equation (25) into equation (23) and integrating with respect to r we obtain:

$$v_z=\frac{N}{m}\Big[\Omega_3(z)K_0(mr)-\Omega_2(z)I_0(mr)\Big]$$
$$+A\left(\frac{r^2}{2}\frac{dp}{dz}+2\Omega_1(z)\ln r\right)+\Omega_4(z),\tag{26}$$

where I_0 and K_0 are the first order modified Bessel functions of zero-order and $\Omega_1,\Omega_2,\Omega_3$ and Ω_4 are constants of integration. From equations (25 and 26) and the boundary conditions (21) the axial and microrotation velocities are given by

$$v_z=-1-\frac{2\pi\alpha\varepsilon\delta\cos(2\pi z)}{1-2\pi\alpha\varepsilon\delta\cos(2\pi z)}$$
$$+\frac{dp}{dz}\{\frac{Ar^2}{2}-\frac{Ah^2}{2}+\frac{AFhI_0(mh)}{2I_1(mh)}-\frac{AFhI_0(mr)}{2I_1(hm)}\},\tag{27}$$

$$w_\theta = \frac{dp}{dz}\{\frac{AhI_1(mr)}{2I_1(mh)} - \frac{Ar}{2}\}, \qquad (28)$$

where $F = \dfrac{n}{m}$.

From equation (17) the stream function can be defined as ($v_z = \dfrac{1}{r}\dfrac{\partial \psi}{\partial r}$ and $v_r = -\dfrac{1}{r}\dfrac{\partial \psi}{\partial z}$),
so the stream function takes the form

$$\psi(r,z) =$$
$$rA\frac{dp}{dz}\{\frac{2mFhrI_0(mh) - 2mh^2 rI_1(mh) + mr^3 I_1(mh) - 4FhI_1(mr)}{8mI_1(mh)}\}$$
$$- \frac{r^2(\dfrac{2\pi\alpha\varepsilon\delta\cos(2\pi z)}{1 - 2\pi\alpha\varepsilon\delta\cos(2\pi z)} + 1)}{2}. \qquad (29)$$

The non-dimensional flux in the moving frame ($q = q' / \pi c a^2$) is given by

$$q = 2\int_0^h rv_z dr =$$
$$-\frac{1}{4}h^2\{4 + \frac{8\pi\alpha\varepsilon\delta\cos(2\pi z)}{1 - 2\pi\alpha\varepsilon\delta\cos(2\pi z)} + \frac{dp}{dz}(Ah^2 + \frac{4AF}{m} - \frac{2AFhI_0(mh)}{I_1(mh)})\}, \qquad (30)$$

from equation (30) the pressure gradient takes the form

$$\frac{dp}{dz} = -\frac{(\dfrac{4q}{h^2} + 4 + \dfrac{8\pi\alpha\varepsilon\delta\cos(2\pi z)}{1 - 2\pi\alpha\varepsilon\delta\cos(2\pi z)})}{Ah^2 + \dfrac{4AF}{m} - \dfrac{2AFhI_0(mh)}{I_1(mh)}}. \qquad (31)$$

The connection between the flow rates in fixed and moving frames over a period is obtained as

$$\overline{Q} = \frac{1}{T}\int_0^T (q + h^2)dt = q + q_1, \qquad (32)$$

where $q_1 = \int_0^1 h^2 dz$. Substituting from equation (32) into (31), we get

$$\frac{dp}{dz} = -\frac{(\dfrac{4(\overline{Q} - q_1)}{h^2} + 4 + \dfrac{8\pi\alpha\varepsilon\cos(2\pi z)}{1 - 2\pi\alpha\varepsilon\cos(2\pi z)})}{Ah^2 + \dfrac{4AF}{m} - \dfrac{2AFhI_0(mh)}{I_1(mh)}}.$$ (33)

The non-dimensional form of the pressure rise Δp takes the form

$$\Delta p = \int_0^1 \frac{dp}{dz} dz,$$ (34)

In the absence of the cilia $(i.e. \ \alpha = 0)$ equations (27-29) take the form

$$v_z = -1 + \frac{1-N}{2(2-N)}\frac{dp}{dz}\left[r^2 - h^2 + \frac{Nr_2}{m}\left(\frac{I_0(mh) - I_0(mr)}{I_1(mh)}\right)\right],$$ (35)

$$w_\theta = \frac{1-N}{2(2-N)}\frac{dp}{dz}\left[\frac{hI_1(mr)}{I_1(mh)} - r\right],$$ (36)

$$\psi(r,z) = -\frac{r^2}{2} +$$
$$\frac{1-N}{2(2-N)}\frac{dp}{dz}\left[\frac{r^4}{4} - \frac{r^2 h^2}{2} + \frac{Nh}{mI_1(mh)}\left(\frac{mr^2 I_0(mh) - 2rI_1(mr)}{2m}\right)\right].$$ (37)

These results are congruent with those obtained by Srinivasacharya [8].

4. Numerical results and discussion

In this section we discuss the effects of sundry parameters that are of relevance to our problem on the axial velocity v_z, microrotation velocity w_θ, pressure gradient $\frac{dp}{dz}$, pressure rise Δp and the stream function $\psi(r,z)$.

4.1. The Axial and microrotation velocities

The effects of the studied parameters on the axial velocity v_z are shown in Figures (2)-(6). While Figures (7)-(11) exhibit the effects of the parameters on the microrotation velocity w_θ.

Figures (2)-(6) Show the variation of the axial velocity v_z with the tube radius r. One can

note that there is a critical value of the tube radius r below which v_z is positive and above which v_z is negative since the maximum value of the fluid velocity takes place at the center of the tube (i. e at $r = 0$), as the tube radius r increases the fluid gets closer to the boundary and consequently the fluid faces a resistance from the boundary and the fluid takes the boundary velocity which is negative according to the boundary condition (21).

Figures (2), (4), (5), and (6) show that effects of the parameters δ, α, N, and m on v_z respectively. It can be noted that below a critical value of r the velocity increases with the increase of the considered parameter (all other parameters are kept constant) and the opposite behavior is noted above such critical value of r. While figure (3) shows that v_z decreases with the increase of the cilia length parameter ε till a critical value of r, then v_z increases with the increase of the cilia length parameter ε after such critical value of r.

As the wave number ($\delta = \dfrac{a}{\lambda}$) increases the wavelength λ decreases assuming that a is fixed, consequently the metachronal waves accelerate the fluid motion till a critical value of r. For values of r greater than such critical value, the effect of δ on v_z is reversed since near the boundary the clia motion is dominant. The effect of increasing the cilia length parameter ε on v_z is to decrease v_z as r increases from 0 till a critical value of r in this region the increase of the cilia length decreases v_z but for values bigger than the critical value of r such effect is reserved (see Figure (3)).

Figure (4) show that the increase of the eccentricity of the elliptical motion α increases the velocity v_z for values of r smaller than a critical value. But for values of r bigger than such critical value v_z decreases with increasing α. Since near the boundary the increase of the eccentricity impedes the fluid motion. In Figure (5), it is shown that the effect of increasing the coupling number N, is to increase the value of v_z for values of r smaller than a critical value, in this region the velocity of the micropolar fluid is greater than that of the Newtonian fluid ($N = 0$) which is justified by the fact that as N increases the effect of micropolar fluid appears more and this accelerates the fluid motion. For values of r greater than the critical value the effect of N is reversed. In figure (6), the effect of the micropolar parameter m is exhibited. One can note that for values of r smaller than a critical value the velocity v_z increases with the increase of m till a critical value of m and then decreases with increasing m. The inverse behavior can be noted for values of r greater than the critical value. Figure (7) shows that as the wave number δ increases the microrotation velocity w_θ decreases this happens because as the wave number δ increases the wavelength decreases which result in pushing the fluid to move along the axis of the tube and hence reduces the microrotation velocity.

It can be observed from Figure (8) that as the cilia length parameter ε increases the radius of the tube decreases for the considered value of z ($z = 0.4$) due to boundary condition (21). The maximum value of w_θ decreases with increasing ε. with r. Figure (9) depicts the effect of the eccentricity parameter of the elliptical motion α on the microrotation velocity

w_{θ}. It is clear that as α elevates the microrotation velocity decreases. In the middle of the tube or near the boundary the effect is limited. The coupling number N has a considerable effect on the microrotation velocity as shown in figure (10). One can see that as N increases (so the fluid goes from Newtonian fluid to micropolar fluid) the microrotation velocity increases. In Figure (11) the microrotation velocity increases with the increase of the micropolar parameter m. One can also note that as m increases the maximum value of the microrotation velocity is shifted to the boundary. That is justified by the fact that near the boundary the concentration of the fluid particles is high which results in increasing the microrotation velocity and ultimately the particle in the vicinity of the boundary do not rotate.

4.2. Pressure Gradient and Pressure Rise

The pressure gradient $\dfrac{dp}{dz}$ is plotted versus z in figures (12)-(16). One can see that the pressure gradient increases with the increase of z reaching a maximum value at a critical value of z. After such critical value the pressure gradient decreases with the increase of z. This behavior can be understood in view of the fact that in the collapsed regions of the tube the pressure gradient elevates to sustain the fluid to move along the tube. while in the wider regions of the tube the pressure gradient decreases. In figure (12) one can see that the pressure gradient decreases with the increase of the wave number δ in the wider regions of the tube. While the pressure gradient increases with the increase of δ in the collapsed regions of the tube. The effect of the cilia length parameter ε on the pressure gradient is shown in figure (13). In case of $\varepsilon = 0$ (Absence of cilia; regular tube) the pressure gradient is fixed along the axis of the tube. While the pressure gradient increases with the increase of the cilia length parameter ε in the narrow regions of the tube, while the converse behavior is noticed in the wider regions of the tube. Figure (14) displays the effect of the eccentricity parameter of the elliptical motion α on the pressure gradient. One can see that the pressure gradient increases with the increase of α in the collapsed regions of the tube. While the converse behavior can be noticed in the wider regions.

The effect of increasing the coupling number N on the pressure gradient is shown in figure (15). One can note that in the case of Newtonian fluid ($N = 0$) the pressure gradient is less than the corresponding values in case of micropolar fluid ($N > 0$). This can be justified by the fact that the coupling between fluid particles requires a raise in pressure gradient in order to accelerate the fluid. Figure (16) shows the effect of the micropolar parameter m on the pressure gradient. It is found that the pressure gradient decreases with the increase of m.

Figure (17) shows that the variation of pressure rise Δp with the cilia length parameter ε for different values of the eccentricity parameter of the elliptical motion α. Such figure shows that as α increases the pressure rise increases. One can also notice that the effect of α does not appear for small values of ε. The figure also shows that with increasing the value of ε the pressure rise increases and this because the occlusion that happens through the tube elevates the pressure rise.

Figure (18) depicts the variation of pressure rise Δp versus δ for different values of the micropolar parameter m. It is clear that the pressure rise decreases as the micropolar parameter increases while it increases as the wave number increases.

Figure (19) shows the variation of the pressure rise Δp with the flow rate $\overline{Q}$ for different values of the coupling number N. It is evident that as the flow rate increases the pressure rise decreases and there is a critical value of the flow rate ($\overline{Q} = 0.161$) this value is known as free pumping flux. Furthermore, we observe that an increase in the coupling number N causes an increase in the magnitude of the pressure rise Δp. This disclosures that the pumping machinery has to function more efficiently to push ahead a micropolar fluid ($N > 0$) in comparison to a Newtonian fluid ($N = 0$).

5. Streamlines and fluid trapping

Trapping is one of the important phenomenon in cilia transport, whereby a bolus is transported with the wave speed. Figure (20) shows the streamline graph for different values of the wave number δ with fixed values of other parameters. It is noticed that both of the size and the number of the trapping bolus increase as the wave number δ increases. The effect of the the cilia length parameter ε on the streamlines is shown in Figure (21). It is clear that as the cilia length parameter ε increases the number of the trapped bolus increases. The effect of the eccentricity parameter of the elliptical motion α on the trapping is illustrated in Figure (22). It is evident that both of the size and number of trapping bolus increase with increasing α.

6. Concluding remarks

A mathematical model is formulated to describe the cilia transport of a micropolar fluid through a uniform cylindrical tube having metachronal waves. The velocity, pressure gradient as well as the stream function are obtained and discussed for various parameters. The fundamental discoveries can be summarized as follows:

- The axial velocity decreases with the increase of the cilia length parameter till a critical value of of the tube radius, then the axial velocity increases with the increase of the cilia length parameter after such critical value.

- The pressure gradient decreases with the increase of the wave number in the wider regions of the tube. While it increases with the increase of the wave number in the collapsed regions of the tube.

- In the case of Newtonian fluid the pressure gradient is less than the corresponding value in case of micropolar fluid.

- The occlusion that happens through the tube elevates the pressure rise.

- Both of the size and the number of the trapping bolus increase as the wave number of the elliptical motion increase.

- Both of the size and the number of the trapping bolus increase as the cilia length parameter increase.

- The pumping machinery functions more efficiently to push ahead micropolar fluid than Newtonian fluid.

REFERENCES

Abd elmaboud Y. (2011). Thermomicropolar fluid flow in a porous channel with peristalsis, Journal of Porous Media, 14 (11) 1033–1045.

Abd elmaboud Y. (2013), Unsteady Flow of Magneto Thermomicropolar Fluid in a Porous Channel With Peristalsis: Unsteady Separation, Journal of Heat Transfer, 135 (7), 072602

Agarwal H. and Anwaruddin (1984). Cilia transport of bio-fluid with variable viscosity, Indian Journal of Pure and Applied Mathematics, 15(10) 1128-1139.

Eringen A.C.(1966). Theory of micropolar fluids, Journal of Mathematics and Mechanics, 16(1) 1-18.

Lardner T. J. and Shack W. J. (1972). Cilia transport, The Bulletin of Mathematical Biophysics, 34(3) 325-335.

Maiti S., Pandey S.K. (2017). Rheological fluid motion in tube by metachronal wave of cilia, Appl. Math. Mech. -Engl. Ed., 38(3), 393–410.

Siddiqui A.M., Farooq A. A., and Rana M. A. (2014 a). Hydromagnetic flow of Newtonian fluid due to ciliary motion in a channel, Magnetohydrodynamics, 50(3)109-122.

Siddiqui A .M., Farooq A. A., and Rana M. A. (2014 b). Study of MHD effects on the cilia-induced flow of a Newtonian fluid through a cylindrical tube, Magetohydrodynamics, 50(4) 249–261.

Siddiqui A. M.,Haroon T. ,Rani M. , and Ansari A. R. (2010). An analysis of the flow of a power law fluid due to ciliary motion in an infinite channel, Journal of Biorheology, 24 (2) 56-69.

Srinivasacharya D., Mishra M., Rao A. R.(2003). Peristaltic pumping of a micropolar fluid in a tube, Acta Mechanica 161, 165-178.

Vijaya B. R., Prasad M. K. and Umadevi C. (2016). A mathematical model for micropolar fluid flow through an artery with the effect of stenosis and post stenotic dilatation, Applications and Applied Mathematics: An International Journal, 11 (2) 680 - 692.
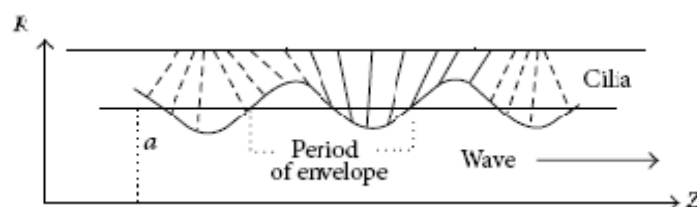
Figure 1. Geometry of the problem
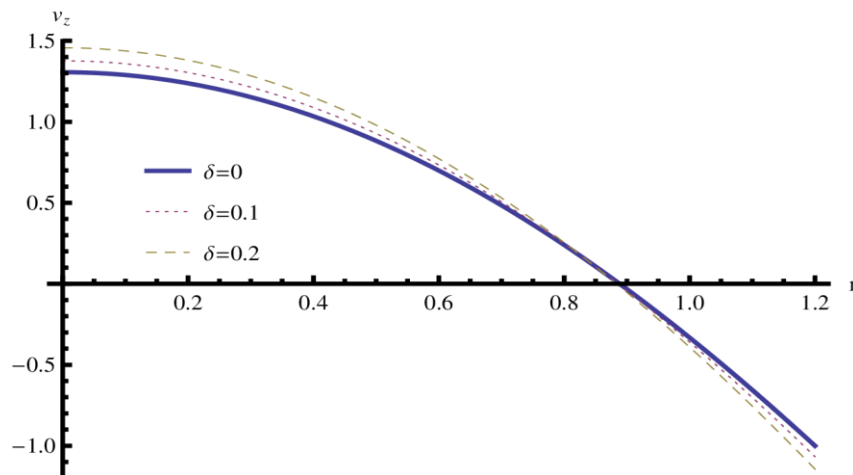
Figure 2. Variation of velocity with r for different values of δ at $\varepsilon = 0.2$, $z = 0$, $\alpha = 0.5$, $\overline{Q} = 1.2$, $m = 2$, $N = 0.5$
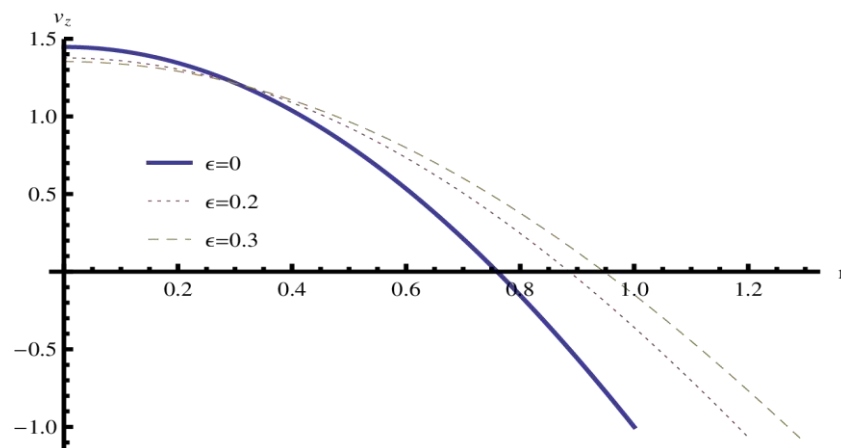
Figure 3. Variation of velocity with r for different values of ε at $\delta = 0.1$, $z = 0$, $\alpha = 0.5$, $\overline{Q} = 1.2$, $m = 2$, $N = 0.5$
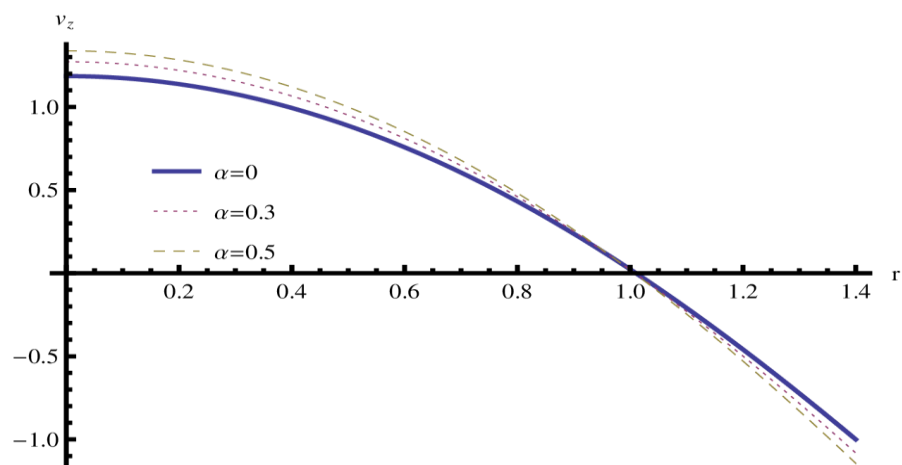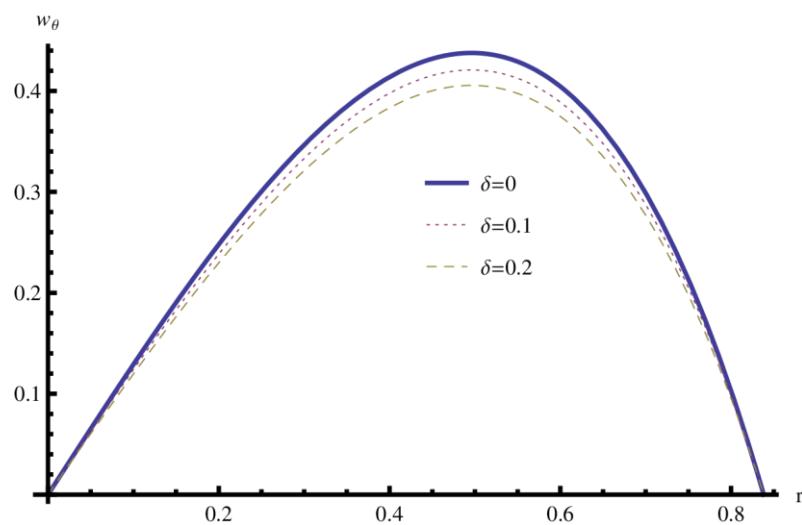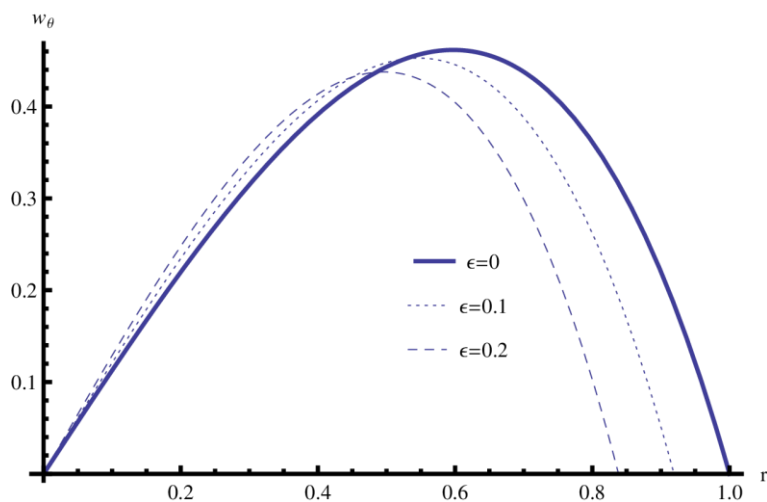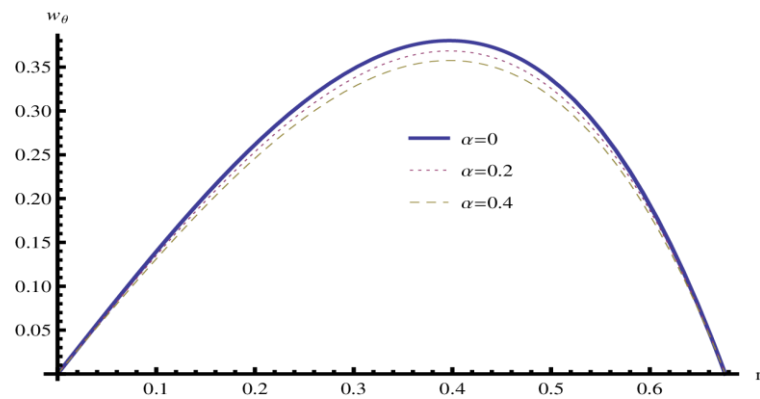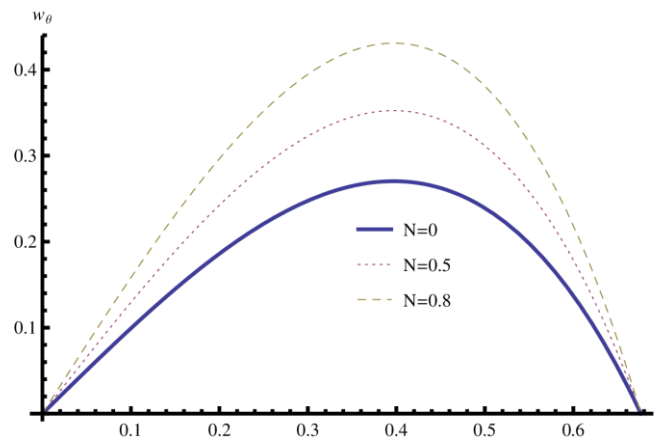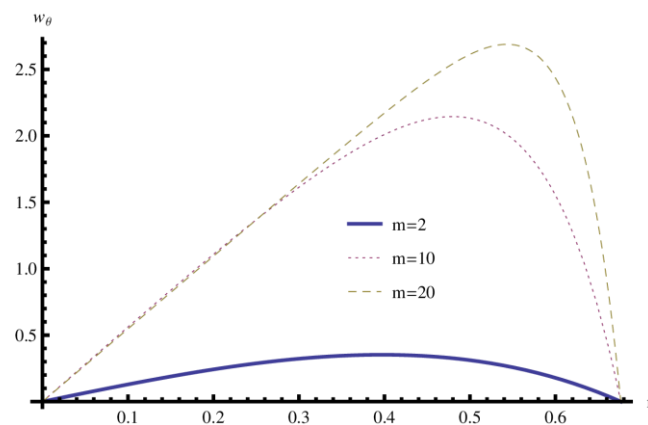

Figure 4. Variation of velocity with r for different values of α at $\delta = 0.1$, $z = 0$, $\varepsilon = 0.4$, $\overline{Q} = 1.2$, $m = 2$, $N = 0.5$
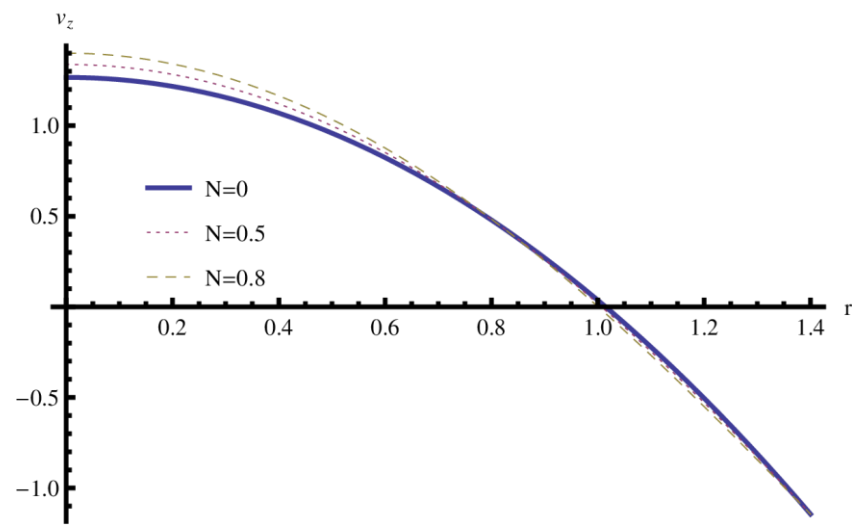
Figure 5. Variation of velocity with r for different values of N at $\delta = 0.1$, $z = 0$, $\varepsilon = 0.4$, $\bar{Q} = 1.2$, $m = 2$, $\alpha = 0.5$
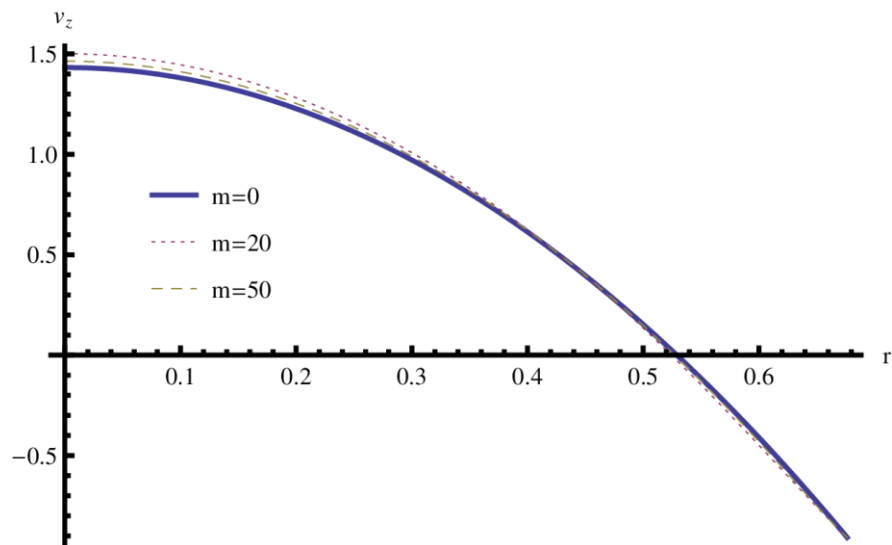
**Figure 6.** Variation of velocity with r for different values of m at $\delta = 0.1$, $z = 0.4$, $\varepsilon = 0.4$, $\bar{Q} = 1,2$, $N = 0.5$, $\alpha = 0.5$

Figure 7. Variation of microrotation velocity with r for different values of δ at $\varepsilon = 0.2$, $z = 0.4$, $\alpha = 0.5$, $\bar{Q} = 1.2$, $m = 2$, $N = 0.5$

Figure 8. Variation of microrotation velocity with r for different values of ε at $\delta = 0.1$, $z = 0.4$, $\alpha = 0.5$, $\bar{Q} = 1.2$, $m = 2$, $N = 0.5$

Figure 9. Variation of microrotation velocity with r for different values of α at $\delta = 0.1$, $z = 0.4$, $\varepsilon = 0.4$, $\bar{Q} = 1.2$, $m = 2$, $N = 0.5$

Figure 10. Variation of microrotation velocity with r for different values of N at $\delta = 0.1$, $z = 0.4$, $\varepsilon = 0.4$, $\bar{Q} = 1.2$, $m = 2$, $\alpha = 0.5$

Figure 11. Variation of microrotation velocity with r for different values of m at $\delta = 0.1$, $z = 0.4$, $\varepsilon = 0.4$, $\bar{Q} = 1,2$, $N = 0.5$, $\alpha = 0.5$
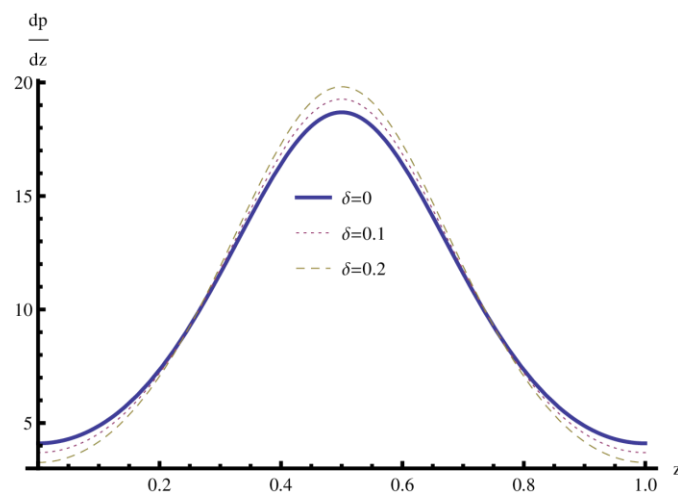
Figure 12. The variation of $\dfrac{dp}{dz}$ with z for different values of δ at $\varepsilon = 0.1$, $\alpha = 0.5$,
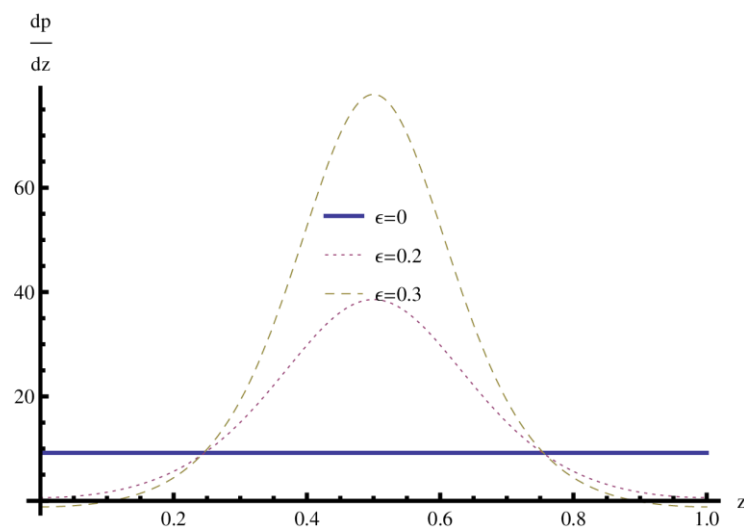
$\bar{Q} = -0.6$, $m = 2$, $N = 0.5$

Figure 13. The variation of $\dfrac{dp}{dz}$ with z for different values of ε at $\delta = 0.1$, $\alpha = 0.5$,
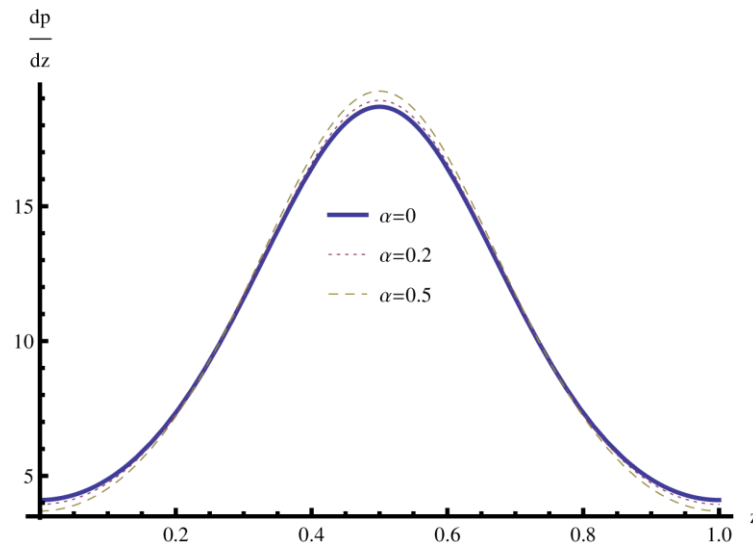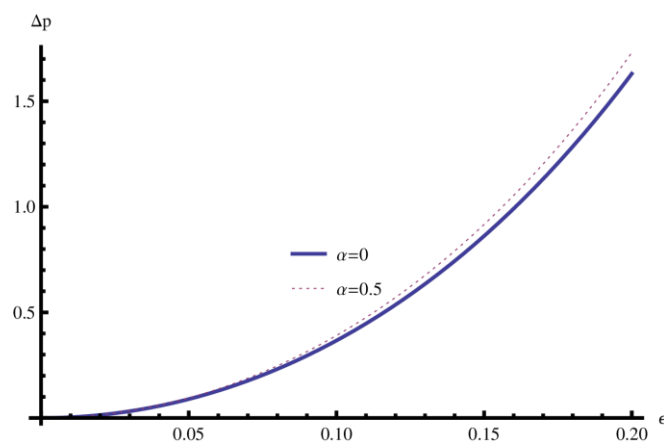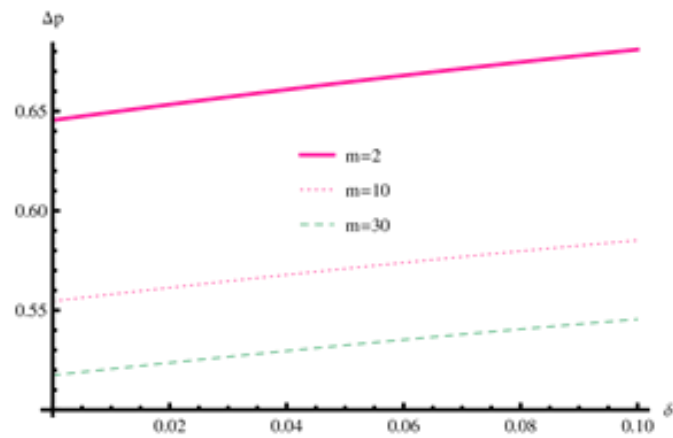
$\bar{Q} = -0.6$, $m = 2$, $N = 0.5$

Figure 14. The variation of $\dfrac{dp}{dz}$ with z for different values of α at $\delta = 0.1$, $\varepsilon = 0.1$, $\overline{Q} = -0.6$, $m = 2$, $N = 0.5$
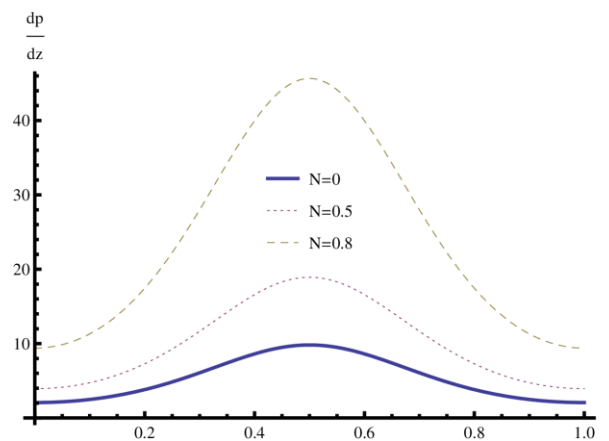
Figure 15. The variation of $\dfrac{dp}{dz}$ with z for different values of N at $\delta = 0.1$, $\varepsilon = 0.1$, $\overline{Q} = -0.6$, $m = 2$, $\alpha = 0.2$
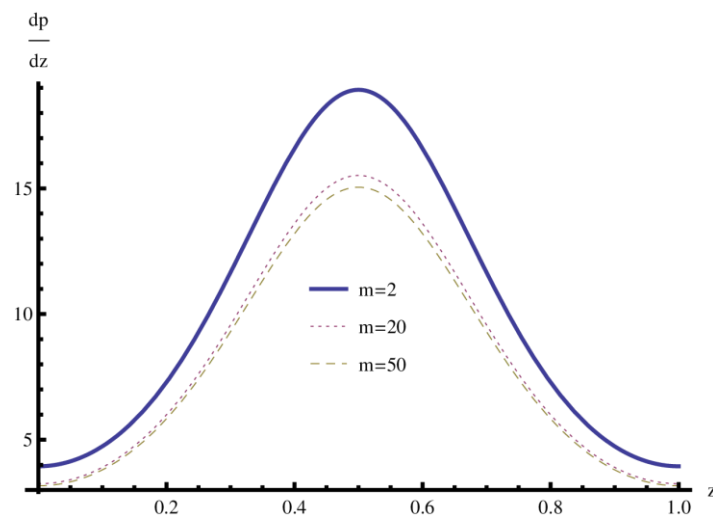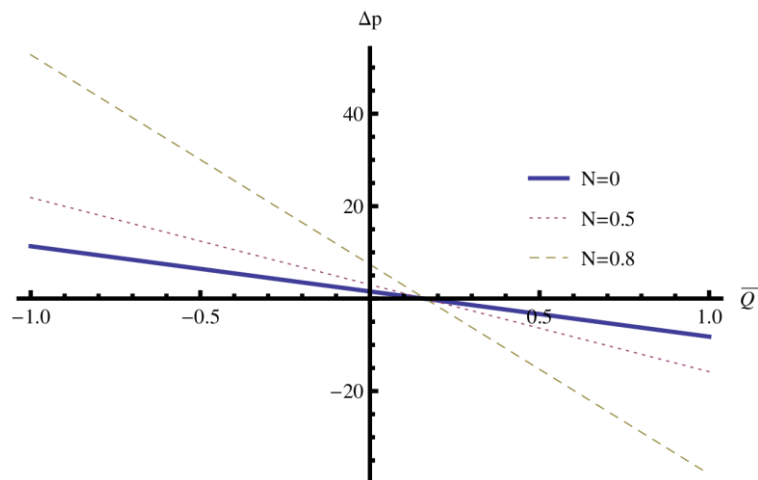
Figure 16. The variation of $\dfrac{dp}{dz}$ with z for different values of m at $\delta = 0.1$, $\varepsilon = 0.1$, $\bar{Q} = -0.6$, $N = 0.5$, $\alpha = 0.2$
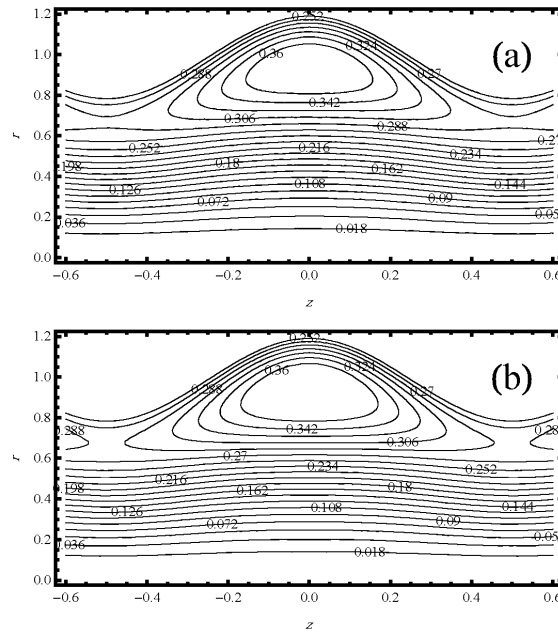

Figure 17. The variation of Δp with ε for different values of α at $\delta = 0.1$, $\bar{Q} = 0$, $m = 2$, $N = 0.5$
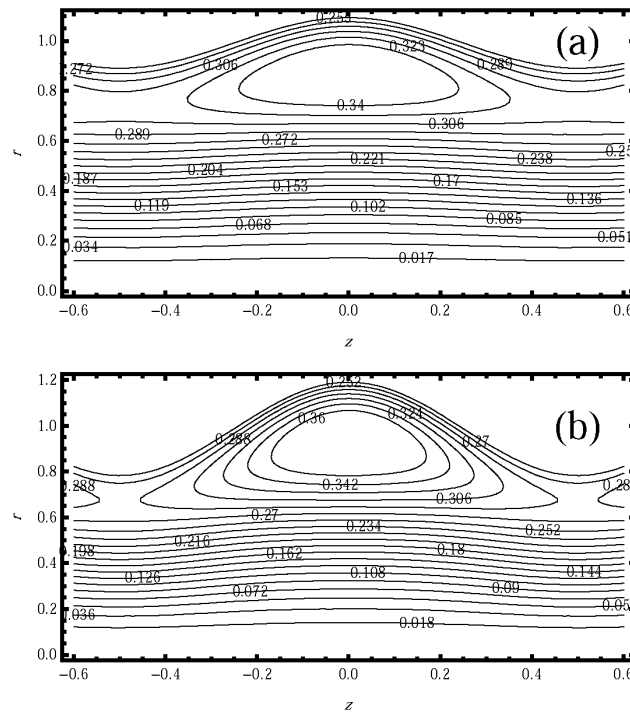
Figure 18. The variation of Δp with δ for different values of m at $\varepsilon = 0.1$, $\bar{Q} = 0$,
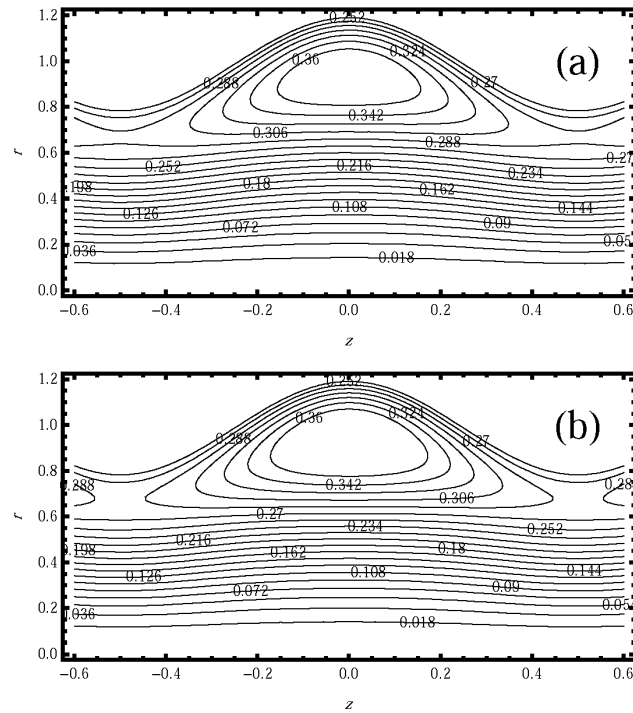$\alpha = 0.4$, $N = 0.5$

Figure 19. The variation of Δp with $\bar{Q}$ for different values of N at $\varepsilon = 0.2$, $\delta = 0.1$,
$\alpha = 0.4$, $m = 2$

Figure 20. Streamlines for different values of δ ($\delta = 0$, $\delta = 0.1$, Panels a,b) with fixed
values of $\alpha = 0.4$, $\overline{Q} = 1.5$, $\varepsilon = 0.2$, $m = 8$, and $N = 0.5$, where
$r \in [0, h(z)]$

Figure 21. Streamlines for different values of ε ($\varepsilon = 0.1$, $\varepsilon = 0.2$, Panels a,b) with
fixed values of $\alpha = 0.4$, $\overline{Q} = 1.5$, $\delta = 0.1$, $m = 8$, and $N = 0.5$, where
$r \in [0, h(z)]$

Figure 22. Streamlines for different values of α ($\alpha = 0$, $\alpha = 0.5$, Panels a,b respectively) with fixed values of $\varepsilon = 0.2$, $\overline{Q} = 1.5$, $\delta = 0.1$, $m = 8$, and $N = 0.5$, where $r \in [0, h(z)]$